SOILS AND FOUNDATIONS Vol. 23, No. 4, Dec. 1983
Japanese Society of Soil Mechanics and Foundation Engineering

CONSTITUTIVE EQUATION FOR SOILS BASED ON THE EXTENDED CONCEPT OF "SPATIAL MOBILIZED PLANE" AND ITS APPLICATION TO FINITE ELEMENT ANALYSIS

TERUO NAKAI* and HAJIME MATSUOKA**

ABSTRACT

A constitutive equation for soils is presented that describes the deformation and strength characteristics of soils in three-dimensional stresses. A stress-strain relationship under shear was developed introducing an extended concept of "Spatial Mobilized Plane" (named the concept of SMP*). In the present paper, paying attention to the fact that the dilatancy of soils under anisotropic consolidation is similar to that under shear, a stress-strain relationship under consolidation is obtained on the basis of the concept of SMP* in the same way as the stress-strain relationship under shear. By combining these two stress-strain relationships and the stress-strain relationship in the elastic state, a generalized constitutive equation is formulated. The validity of this proposed constitutive equation is checked by the analysis of various kinds of element tests and its comparison with the experimental results. All the soil parameters of the proposed constitutive equation can be determined from shear and consolidation tests by using a conventional triaxial compression test apparatus.

Finite element analyses for bearing capacity problems are then performed by using the proposed constitutive equation. The analytical results explain well various deformation and failure behaviors of soil foundation which have been well-known empirically.

Key words: bearing capacity, clay, constitutive equation of soil, dilatancy, finite element method, laboratory test, sand, shallow foundation, shear strength, stress path, stress-strain curve (**IGC**: D 6/E 0/E 3)

INTRODUCTION

Since Roscoe et al. (1963) proposed the Cam-clay model, a number of constitutive models for soils which can be applied to the finite element analysis of soil foundations and earth structures have been developed. Most of these models are based on the theory of plasticity with strain hardening. For example, Ohta (1971) and Sekiguchi and Ohta (1977) extended the Cam-clay model so as to explain the behavior of anisotropically

* Associate Professor, Department of Civil Engineering, Nagoya Institute of Technology, Gokiso-cho, Showa-ku, Nagoya.
** Associate Professor, Department of Civil Engineering, Nagoya Institute of Technology, Gokiso-cho, Showa-ku, Nagoya.
Manuscript was received for review on March 23, 1983.
Written discussions on this paper should be submitted before October 1, 1984.

consolidated clay. Pender (1977) proposed a unified model for normally consolidated and over-consolidated clays by assuming two yield functions and two plastic potential functions. Prévost (1978) explained cyclic stress-strain behavior of clay combining isotropic and kinematic hardening rules. Moreover, viscoplastic models considering time-dependent behavior of clay were developed by Adachi and Okano (1974), Sekiguchi (1977), Oka (1981) and others. By the way, these above-stated models did not take the effect of intermediate principal stress into account precisely, because these were made mainly referring to the results of triaxial compression tests. Lade and Duncan (1973, 1975) performed true triaxial tests on sand, and developed an elastoplastic model for sand in which the effect of intermediate principal stress was considered.

The authors proposed the "Spatial Mobilized Plane (SMP)" as the plane where soil particles are most mobilized on the average in the three-dimensional space, and developed a stress-strain relationship under shear based on this SMP (Matsuoka and Nakai, 1974, 1977). By introducing new amounts of strain increments based on the SMP, they proposed another stress-strain relationship which explained shear behavior of soil more uniquely (Nakai and Matsuoka, 1980, 1983). This is named the stress-strain relationship based on the concept of SMP*. In the present paper, taking note of the fact that the soil behavior under anisotropic consolidation is similar to that under shear, a stress-strain relationship under consolidation is formulated based on the concept of SMP*, as well as under shear. Further, by considering the elastic component besides these shear and consolidation components, a generalized constitutive model is presented that can explain uniquely the soil behavior under various stress paths in three-dimensional stresses. The proposed model is obtained not using directly the yield function, the plastic potential function and the strain-hardening function which are employed in the theory of plasticity. After the validity of the model is confirmed by the various analyses of soil element tests, the model is applied to the finite element analysis of soil-footing interaction problem and the analytical results are compared with those of stability analysis.

CONSTITUTIVE EQUATION FOR SOILS

The total strain increments of soil $\{d\varepsilon\}$ are generally expressed as the summation of the plastic component $\{d\varepsilon^p\}$ and the elastic component $\{d\varepsilon^e\}$. In this study, considering that the plastic strain increments can be divided into the plastic strain increments due to shear $\{d\varepsilon^s\}$ (the strain increments caused by an increase in stress ratio) and the plastic strain increments due to consolidation $\{d\varepsilon^c\}$ (the strain increments caused by an increase in mean principal stress), the total strain increments in the general coodinate system are expressed as follows:

$$\begin{aligned}\{d\varepsilon\} &= \{d\varepsilon^p\} + \{d\varepsilon^e\} \\ &= \{d\varepsilon^s\} + \{d\varepsilon^c\} + \{d\varepsilon^e\} \end{aligned} \quad (1)$$

Throughout this paper, the superscript p denotes the plastic component, e the elastic component, s the plastic component due to shear and c the plastic component due to consolidation.

Plastic Strain Increments due to Shear $\{d\varepsilon^s\}$

In soil mechanics, the strain due to shear is defined to be the strain caused by an increase in the stress ratio under constant mean principal stress. The stress-strain relationship under shear has been derived introducing the new concept of "Spatial Mobilized Plane* (SMP*)" by the authors (Nakai and Matsuoka, 1980, 1983). The outline of this stress-strain relationship is described as follows.

Fig. 1 shows a soil element and the Spatial Mobilized Plane (SMP) in three-dimensional space, where I, II and III axes represent the directions to which three principal stresses σ_1, σ_2 and σ_3 are applied, respectively. Here, the SMP has been considered to be the plane where soil particles are most mobilized on the average, and its direction cosines

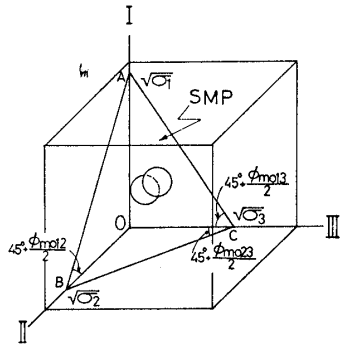

Fig. 1. A soil element and Spatial Mobilized Plane (ABC) in three-dimensional space

are expressed as follows:

$$a_i=\sqrt{\frac{J_3}{\sigma_i\cdot J_2}}\quad(i=1,2,3)\qquad(2)$$

where J_1, J_2 and J_3 are the first, second and third effective stress invariants and expressed by the following equations using the principal stresses (σ_1, σ_2 and σ_3) or the stresses in the general coordinate system ($\sigma_x, \sigma_y, \sigma_z, \tau_{xy}, \tau_{yz}$ and τ_{zx}).

$$\left.\begin{aligned}J_1&=\sigma_1+\sigma_2+\sigma_3=\sigma_x+\sigma_y+\sigma_z\\J_2&=\sigma_1\sigma_2+\sigma_2\sigma_3+\sigma_3\sigma_1\\&=\sigma_x\sigma_y+\sigma_y\sigma_z+\sigma_z\sigma_x-\tau_{xy}^2-\tau_{yz}^2-\tau_{zx}^2\\J_3&=\sigma_1\sigma_2\sigma_3\\&=\sigma_x\sigma_y\sigma_z+2\tau_{xy}\tau_{yz}\tau_{zx}-\sigma_x\tau_{yz}^2\\&\quad-\sigma_y\tau_{zx}^2-\sigma_z\tau_{xy}^2\end{aligned}\right\}\qquad(3)$$

According to the concept of SMP*, there are the following two basic equations uniquely between the shear-normal stress ratio on the SMP ($X\equiv\tau_{SMP}/\sigma_{SMP}$) and the new amounts of strain increments ($d\varepsilon_{SMP}{}^{*s}$ and $d\gamma_{SMP}{}^{*s}$) which denote the normal and parallel components of the principal strain increment vector to the SMP.

$$X\equiv\frac{\tau_{SMP}}{\sigma_{SMP}}=\lambda\left(-\frac{d\varepsilon_{SMP}{}^{*s}}{d\gamma_{SMP}{}^{*s}}\right)+\mu^*\qquad(4)$$

$$X\equiv\frac{\tau_{SMP}}{\sigma_{SMP}}=\lambda\left(-\frac{\varepsilon_{SMP}{}^{*s}}{\gamma_{SMP}{}^{*s}}\right)+\mu'^*\qquad(5)$$

$$\left(\varepsilon_{SMP}{}^{*s}=\int d\varepsilon_{SMP}{}^{*s},\ \gamma_{SMP}{}^{*s}=\int d\gamma_{SMP}{}^{*s}\right)$$

where the shear-normal stress ratio on the SMP $X\equiv\tau_{SMP}/\sigma_{SMP}$ is given as follows using the stress invariants:

$$X\equiv\frac{\tau_{SMP}}{\sigma_{SMP}}=\sqrt{\frac{J_1J_2-9J_3}{9J_3}}\qquad(6)$$

By solving the differential equation obtained from Eqs. (4) and (5), the following equation is derived.

$$\gamma_{SMP}{}^{*s}=\gamma_0\cdot\exp\left(\frac{X-\mu^*}{\mu'^*-\mu^*}\right)\qquad(7)$$

Therefore, from Eqs. (4) and (7), $d\gamma_{SMP}{}^{*s}$ and $d\varepsilon_{SMP}{}^{*s}$ are given as functions of the stress ratio.

$$\begin{aligned}d\gamma_{SMP}{}^{*s}&=\frac{\gamma_0^*}{\mu'^*-\mu^*}\cdot\exp\left(\frac{X-\mu^*}{\mu'^*-\mu^*}\right)\cdot dX\\&\equiv G_1^*\cdot dX\end{aligned}\qquad(8)$$

$$\begin{aligned}d\varepsilon_{SMP}{}^{*s}&=\frac{\mu^*-X}{\lambda^*}\cdot d\gamma_{SMP}{}^{*s}=\frac{\mu^*-X}{\lambda^*}\cdot G_1^*\cdot dX\\&\equiv E_1^*\cdot dX\end{aligned}\qquad(9)$$

In these equations, each of the soil parameters λ^*, μ^* and μ'^* is considered to be nearly constant for a given sample. On the other hand, the parameter γ_0^* is considered to be a function of effective mean principal stress σ_m, and is empirically expressed as follows:

$$\gamma_0^*=\gamma_{0i}^*+C_d^*\cdot\log_{10}(\sigma_m/\sigma_{mi})\qquad(10)$$

The direction cosines of $d\varepsilon_{SMP}{}^{*s}$ is equal to a_i ($i=1,2,3$) given by Eq. (2), on the assumption that the direction of the principal stresses and that of the plastic principal strain increments are identical. If $d\gamma_{SMP}{}^{*s}$ is assumed to coincide with the shear stress on the SMP (τ_{SMP}) in direction, the direction cosines of $d\gamma_{SMP}{}^{*s}$ are expressed by the following direction cosines of τ_{SMP}.

$$b_i=\frac{\sigma_i-\sigma_{SMP}}{\tau_{SMP}}\cdot a_i=\frac{\sigma_iJ_2-3J_3}{\sqrt{\sigma_iJ_2(J_1J_2-9J_3)}}\quad(i=1,2,3)\qquad(11)$$

Therefore, the plastic principal strain increments due to shear $d\varepsilon_i{}^s$ can be given by the following equations.

$$\begin{aligned}d\varepsilon_i{}^s&=a_i\cdot d\varepsilon_{SMP}{}^{*s}+b_i\cdot d\gamma_{SMP}{}^{*s}\\&=(a_i\cdot E_1^*+b_i\cdot G_1^*)\cdot dX\\&\equiv E_i{}^s\cdot dX\quad(i=1,2,3)\end{aligned}\qquad(12)$$

or

$$\{d\varepsilon_i{}^s\}=\{E_i{}^s\}\cdot dX\qquad(13)$$

Now, performing the total differentiation of Eq. (6), the shear-normal stress ratio

increment on the SMP (dX) is represented as follows by using the general stress increments $\{d\sigma\}=[\sigma_x, \sigma_y, \sigma_z, \tau_{xy}, \tau_{yz}, \tau_{zx}]^T$:

$$dX=\left\{\frac{\partial X}{\partial \sigma}\right\}^T\cdot\{d\sigma\}$$
$$=\frac{1}{18XJ_3^2}$$
$$\left\{\begin{array}{l} J_2J_3+J_1J_3(\sigma_y+\sigma_z)-J_1J_2(\sigma_y\sigma_z-\tau_{yz}^2) \\ J_2J_3+J_1J_3(\sigma_z+\sigma_x)-J_1J_2(\sigma_z\sigma_x-\tau_{zx}^2) \\ J_2J_3+J_1J_3(\sigma_x+\sigma_y)-J_1J_2(\sigma_x\sigma_y-\tau_{xy}^2) \\ \quad -2J_1J_3\tau_{xy}-2J_1J_2(\tau_{yz}\tau_{zx}-\sigma_z\tau_{xy}) \\ \quad -2J_1J_3\tau_{yz}-2J_1J_2(\tau_{zx}\tau_{xy}-\sigma_x\tau_{yz}) \\ \quad -2J_1J_3\tau_{zx}-2J_1J_2(\tau_{xy}\tau_{yz}-\sigma_y\tau_{zx}) \end{array}\right\}^T$$
$$\cdot\{d\sigma\}\equiv\{A\}^T\cdot\{d\sigma\} \qquad (14)$$

The superscript T denotes the transposition of matrix. From Eqs. (13) and (14), the plastic principal strain increments due to shear $\{d\varepsilon_i^s\}=[d\varepsilon_1^s,\ d\varepsilon_2^s,\ d\varepsilon_3^s]^T$ are expressed by the following formula using the general stress increments $\{d\sigma\}$.

$$\{d\varepsilon_i^s\}=\{E_i^s\}\cdot\{A\}^T\cdot\{d\sigma\} \qquad (15)$$

Then, introducing the matrix $[T]$ which transforms the principal strain increments into the general strain increments, the general plastic strain increments due to shear $\{d\varepsilon^s\}=[d\varepsilon_x^s,\ d\varepsilon_y^s,\ d\varepsilon_z^s,\ d\gamma_{xy}^s,\ d\gamma_{yz}^s,\ d\gamma_{zx}^s]^T$ can be represented as follows by using the general stress increments $\{d\sigma\}$.

$$\{d\varepsilon^s\}=[T]\cdot\{d\varepsilon_i^s\}$$
$$=[T]\cdot\{E_i^s\}\cdot\{A\}^T\cdot\{d\sigma\} \qquad (16)$$

The transformation matrix $[T]$ is given as a formula of stresses on the assumption that the direction of the plastic principal strain increments and that of the principal stresses are identical.

$$[T]=\begin{bmatrix} l_x^2 & m_x^2 & n_x^2 \\ l_y^2 & m_y^2 & n_y^2 \\ l_z^2 & m_z^2 & n_z^2 \\ 2l_xl_y & 2m_xm_y & 2n_xn_y \\ 2l_yl_z & 2m_ym_z & 2n_yn_z \\ 2l_zl_x & 2m_zm_x & 2n_zn_x \end{bmatrix} \qquad (17)$$

where (l_x, l_y and l_z) denote the direction cosines of σ_1-axis to the x, y and z axes, respectively, and are expressed as,

$$\left.\begin{array}{l} l_x=\dfrac{1}{D_1}\{(\sigma_1-\sigma_y)\tau_{zx}+\tau_{xy}\tau_{yz}\} \\ l_y=\dfrac{1}{D_1}\{(\sigma_1-\sigma_x)\tau_{yz}+\tau_{xy}\tau_{zx}\} \\ l_z=\dfrac{1}{D_1}\{(\sigma_1-\sigma_x)(\sigma_1-\sigma_y)-\tau_{xy}^2\} \end{array}\right\} \qquad (18)$$

in which

$$D_1=\sqrt{\{(\sigma_1-\sigma_y)\tau_{zx}-\tau_{xy}\tau_{yz}\}^2+\{(\sigma_1-\sigma_x)\tau_{yz}+\tau_{xy}\tau_{zx}\}^2+\{(\sigma_1-\sigma_x)(\sigma_1-\sigma_y)-\tau_{xy}^2\}^2} \qquad (19)$$

(m_x, m_y and m_z) represent the direction cosines of σ_2-axis and (n_x, n_y and n_z) the direction cosines of σ_3-axis, and these direction cosines are expressed by replacing σ_1 in Eqs. (18) and (19) with σ_2 and σ_3, respectively. The transformation matrix $[T]$ under plane strain condition is shown in Appendix.

Plastic Strain Increments due to Consolidation $\{d\varepsilon^c\}$

The plastic strain due to consolidation is considered to be the plastic strain caused by

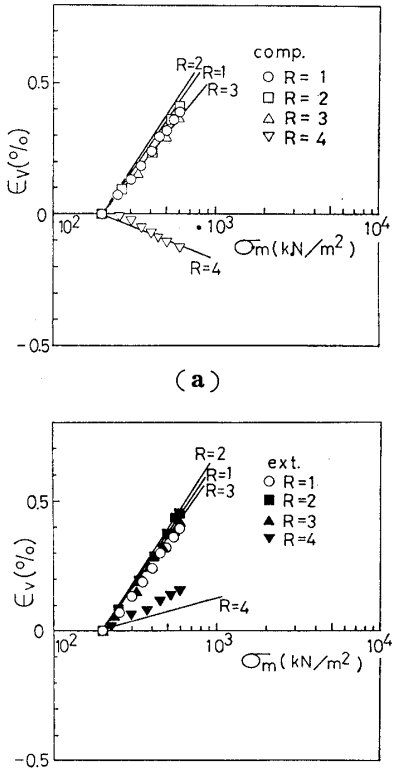

(a)

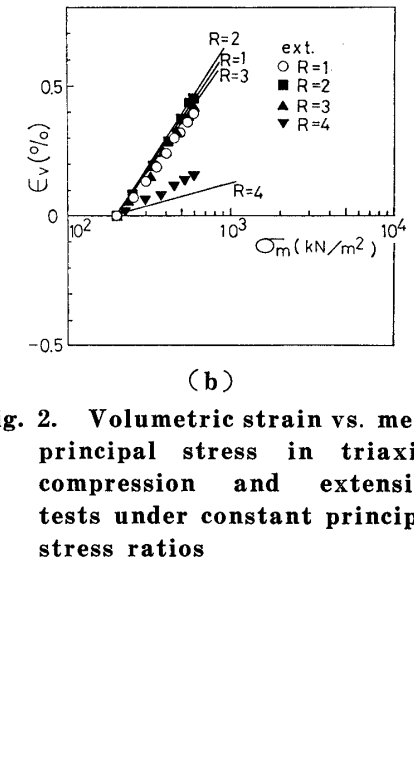

(b)

Fig. 2. Volumetric strain vs. mean principal stress in triaxial compression and extension tests under constant principal stress ratios

an increase in the mean principal stress under constant stress ratio. Here, upon the consideration about anisotropic consolidation tests of soils, the plastic strain increment due to consolidation will be formulated.

The plots in Figs. 2(a) and 2(b) indicate the test results of anisotropic consolidation tests on medium dense Toyoura sand (initial void ratio $e_0 \cong 0.68$) under triaxial compression and triaxial extension conditions respectively, with respect to the relation between volumetric strain ε_v and $\log_{10}\sigma_m$ (σ_m: effective mean principal stress). R denotes the major-minor principal stress ratio σ_1/σ_3. The volumetric strain due to consolidation ε_v has hitherto been expressed by the following equation regardless of the stress ratio, as represented in Cam-clay model and so on(e. g., Schofield and Wroth, 1968).

$$\varepsilon_v = \frac{C_c}{1+e_0} \log_{10} \frac{\sigma_m}{\sigma_{m0}} \tag{20}$$

where C_c is the compression index, e_0 the initial void ratio and σ_{m0} the initial mean principal stress. However, it is observed from these figures that the validity of Eq. (20) is limited to the isotropic consolidation and anisotropic consolidation under low stress ratio. Strictly investigated, ε_v in anisotropic consolidation tests under low stress ratios ($R=2$ and 3) is slightly compressive in comparison with ε_v in isotropic consolidation test ($R=1$), and ε_v in anisotropic consolidation tests under high stress ratio ($R=4$) is expansive in comparison with ε_v in $R=1$ test. Moreover, ε_v in $R=4$ test is more expansive under triaxial compression condition than under triaxial extension condition. Test results of sand with such tendencies were also reported by El-Sohby (1964). Now, since these characteristics of volumetric strain which are expressed as the difference between the isotropic consolidation test and each of the anisotropic consolidation tests are similar to the soil dilatancy under shear (see Fig. 22 in another paper by Nakai and Matsuoka (1983)), in the current study the strains due to consolidation are assumed to be divisible into the component under isotropic consolidation and the component due to dilatancy under anisotropic consolidation (Nakai and Matsuoka, 1981).

The plastic principal strain increments due to isotropic consolidation $d\varepsilon_{i\,(\mathrm{iso})}{}^c$ are given by the following equation with reference to Eq. (20):

$$d\varepsilon_{i\,(\mathrm{iso})}{}^c = \frac{0.434}{3} \cdot \frac{C_c - C_s}{1+e_0} \cdot \frac{d\sigma_m}{\sigma_m} \quad (i=1,2,3) \tag{21}$$

where C_s is the swelling index.

The plastic principal strain increments due to dilatancy under anisotropic consolidation $d\varepsilon_{i\,(\mathrm{dil})}{}^c$ are determined as follows using the new concept of SMP*, since the soil dilatancies under both shear and anisotropic consolidation have similar characteristics. Firstly, considering that no shear strain is produced under isotropic stress condition, Eq. (7) is modified as

$$\gamma_{\mathrm{SMP}}{}^* = \gamma_0{}^* \left\{ \exp\left(\frac{X-\mu^*}{\mu'^*-\mu^*} \right) - \exp\left(\frac{-\mu^*}{\mu'^*-\mu^*} \right) \right\} \tag{22}$$

Next, by performing total differentiation of Eq. (22) in consideration of the condition that soil parameter $\gamma_0{}^*$ is expressed by Eq. (10) as a function of mean principal stress σ_m, the following equation can be obtained.

$$\begin{aligned} d\gamma_{\mathrm{SMP}}{}^* = {} & \frac{\gamma_0{}^*}{\mu'^*-\mu^*} \exp\left(\frac{X-\mu^*}{\mu'^*-\mu^*} \right) \cdot dX \\ & + 0.434 \cdot C_d{}^* \cdot \left\{ \exp\left(\frac{X-\mu^*}{\mu'^*-\mu^*} \right) \right. \\ & \left. - \exp\left(\frac{-\mu^*}{\mu'^*-\mu^*} \right) \right\} \cdot \frac{d\sigma_m}{\sigma_m} \end{aligned} \tag{23}$$

As the first term of right side in Eq. (23) is the same as the amount of strain increment due to shear $d\gamma_{\mathrm{SMP}}{}^{*s}$ which is expressed by Eq. (8), the second term may be regarded as the amount of strain increment due to anisotropic consolidation $d\gamma_{\mathrm{SMP}}{}^{*c}$. Eq. (23) implies that $\gamma_{\mathrm{SMP}}{}^*$ is the quantity of state which is independent of the stress paths because it is in the total differential form with respect to X and σ_m. However, $\gamma_{\mathrm{SMP}}{}^*$ depends on the stress path, according to the test results (Nakai and Matsuoka, 1981). So, in order to evaluate the stress path dependency of $\gamma_{\mathrm{SMP}}{}^*$, the amount of strain increment $d\gamma_{\mathrm{SMP}}{}^{*c}$ is given by the

following equation replacing C_d^* in the second term of Eq. (23) with a different coefficient K_c.

$$d\gamma_{SMP}^{*c}=0.434\cdot K_c\cdot\left\{\exp\left(\frac{X-\mu^*}{\mu'^*-\mu^*}\right)-\exp\left(\frac{-\mu^*}{\mu'^*-\mu^*}\right)\right\}\frac{d\sigma_m}{\sigma_m}\equiv G_2^*\cdot d\sigma_m \quad (24)$$

The method to determine K_c will be discussed later. Another amount of strain increment due to anisotropic consolidation $d\varepsilon_{SMP}^{*c}$ is expressed by the following equation, since the component due to dilatancy under anisotropic consolidation is considered to satisfy the stress ratio-strain increment ratio relation of Eq. (4) in the same way as under shear.

$$d\varepsilon_{SMP}^{*c}=\frac{\mu^*-X}{\lambda^*}\cdot d\gamma_{SMP}^{*c}=\frac{\mu^*-X}{\lambda^*}\cdot G_2^*\cdot d\sigma_m\equiv E_2^*\cdot d\sigma_m \quad (25)$$

Therefore, the plastic principal strain increments due to dilatancy under anisotropic consolidation $d\varepsilon_{i(dil)}^c$ are given as follows in the same manner as Eq. (12):

$$d\varepsilon_{i(dil)}^c=a_i\cdot d\varepsilon_{SMP}^{*c}+b_i\cdot d\gamma_{SMP}^{*c}=(a_i\cdot E_2^*+b_i\cdot G_2^*)\cdot d\sigma_m \quad (26)$$

The plastic principal strain increments due to consolidation $d\varepsilon_i^c$ can be expressed as the summation of $d\varepsilon_{i(iso)}^c$ and $d\varepsilon_{i(dil)}^c$.

$$d\varepsilon_i^c=d\varepsilon_{i(iso)}^c+d\varepsilon_{i(dil)}^c=\left(\frac{0.434}{3}\cdot\frac{C_c-C_s}{(1+e_0)\sigma_m}+a_i\cdot E_2^*+b_i\cdot G_2^*\right)\cdot d\sigma_m\equiv E_i^c\cdot d\sigma_m \quad (i=1,2,3) \quad (27)$$

or

$$\{d\varepsilon_i^c\}=\{E_i^c\}\cdot d\sigma_m \quad (28)$$

where $\{d\varepsilon_i^c\}=[d\varepsilon_1^c,\ d\varepsilon_2^c,\ d\varepsilon_3^c]^T$ and $\{E_i^c\}=[E_1^c,\ E_2^c,\ E_3^c]^T$

Here, $d\sigma_m$ is represented as follows using the general stress increments $\{d\sigma\}$:

$$d\sigma_m=[1/3,\ 1/3,\ 1/3,\ 0,\ 0,\ 0]\cdot\{d\sigma\}\equiv\{B\}^T\cdot\{d\sigma\} \quad (29)$$

Therefore, using the transformation matrix $[T]$ expressed by Eq. (17), the general plastic strain increments due to consolidation $\{d\varepsilon^c\}=[d\varepsilon_x^c,\ d\varepsilon_y^c,\ d\varepsilon_z^c,\ d\gamma_{xy}^c,\ d\gamma_{yz}^c,\ d\gamma_{zx}^c]^T$ can be given by the following equation from Eqs. (28) and (29).

$$\{d\varepsilon^c\}=[T]\cdot\{d\varepsilon_i^c\}=[T]\cdot\{E_i^c\}\cdot\{B\}^T\cdot\{d\sigma\} \quad (30)$$

Elastic Strain Increments $\{d\varepsilon^e\}$

The elastic strain increments $\{d\varepsilon^e\}=[d\varepsilon_x^e,\ d\varepsilon_y^e,\ d\varepsilon_z^e,\ d\gamma_{xy}^e,\ d\gamma_{yz}^e,\ d\gamma_{zx}^e]^T$ are given using the incremental stress-strain relationship for an isotropic elastic material.

$$\{d\varepsilon^e\}=\frac{1}{E_e}\begin{bmatrix}1&-\nu_e&-\nu_e&0&0&0\\-\nu_e&1&-\nu_e&0&0&0\\-\nu_e&-\nu_e&1&0&0&0\\0&0&0&2(1+\nu_e)&0&0\\0&0&0&0&2(1+\nu_e)&0\\0&0&0&0&0&2(1+\nu_e)\end{bmatrix}\cdot\{d\sigma\}\equiv[D_e]^{-1}\cdot\{d\sigma\} \quad (31)$$

in which E_e is the tangential Young's modulus and ν_e the Poisson's ratio. In Eq. (31), E_e is determined as follows using the swelling index C_s in e vs. $\log_{10}\sigma_m$ relation.

$$E_e=3(1-2\nu_e)\cdot K_e=\frac{3(1-2\nu_e)(1+e_0)\sigma_m}{0.434\cdot C_s} \quad (32)$$

where K_e is the bulk modulus.

By the way, the coefficient K_c in Eq. (24) is determined as follows by using the K_0 value and the soil parameter on the condition that constitutive equation proposed here satisfies the K_0-consolidation state. Since the principal strain increments $d\varepsilon_2$ and $d\varepsilon_3$ are equal to zero at the K_0-consolidation state ($\sigma_1/\sigma_3=1/K_0$, $\sigma_2=\sigma_3$), the following equation is obtained.

$$d\varepsilon_3=d\varepsilon_3^c+d\varepsilon_3^e=0 \quad (33)$$

In Eq. (33), $d\varepsilon_3^c$ and $d\varepsilon_3^e$ are expressed as follows from Eqs. (27) and (31), respectively.

$$d\varepsilon_3^c=\left(\frac{0.434}{3}\cdot\frac{C_c-C_s}{(1+e_0)\sigma_m}+a_{3\cdot0}\cdot E_2^*+b_{3\cdot0}\cdot G_2^*\right)d\sigma_m \quad (34)$$

$$d\varepsilon_3^e=\frac{1}{E_e}\{d\sigma_3-\nu_e(d\sigma_1+d\sigma_3)\}=\frac{1}{E_e}\{K_0-(1+K_0)\nu_e\}\cdot\frac{3}{1+2K_0}\cdot d\sigma_m$$

$$=\frac{0.434\{K_0-(1+K_0)\nu_e\}}{(1-2\nu_e)(1+2K_0)}\frac{C_s}{(1+e_0)\sigma_m}\cdot d\sigma_m \tag{35}$$

By substituting Eqs. (34) and (35) into Eq. (33) and rearranging the formula, the coefficient K_c is given as a function of the K_0 value and the soil parameters.

$$K_c=\frac{-\left[\dfrac{C_c-C_s}{3(1+e_0)}+\dfrac{\{K_0-(1+K_0)\nu_e\}C_s}{(1-2\nu_e)(1+2K_0)(1+e_0)}\right]}{\left\{\exp\left(\dfrac{X_0-\mu}{\mu'^*-\mu^*}\right)-\exp\left(\dfrac{-\mu^*}{\mu'^*-\mu^*}\right)\right\}\left\{\dfrac{\mu^*-X_0}{\lambda^*}\cdot a_{3\cdot0}+b_{3\cdot0}\right\}} \tag{36}$$

In the above equations, X_0, $a_{3\cdot0}$ and $b_{3\cdot0}$ represent the shear-normal stress ratio on the SMP τ_{SMP}/σ_{SMP}, the direction cosine of σ_{SMP} to the σ_3-axis, and the direction cosine of τ_{SMP} to the σ_3-axis on the condition of K_0-consolidation, respectively, and expressed as follows from Eqs. (6), (2) and (11).

$$X_0=\frac{\sqrt{2}}{3}(\sqrt{\sigma_1/\sigma_3}-\sqrt{\sigma_3/\sigma_1})=\frac{\sqrt{2}}{3}(\sqrt{1/K_0}-\sqrt{K_0}) \tag{37}$$

$$a_{3\cdot0}=\sqrt{J_3/(\sigma_3 J_2)}=\sqrt{1/(2+K_0)} \tag{38}$$

$$b_{3\cdot0}=\frac{\sigma_3-\sigma_{SMP}}{\tau_{SMP}}\cdot a_{3\cdot0}=-\sqrt{K_0/(4+2K_0)} \tag{39}$$

Explicit Representation of the Constitutive Equation

The method to represent the constitutive equation described above in an explicit form such as $\{d\sigma\}=[D]\cdot\{d\varepsilon\}$ ($[D]$: stress-strain matrix), will be discussed here with reference to the procedure by Yamada et al. (1968) in the elastoplastic theory. The following equation holds from Eqs. (1), (16), (30) and (31).

$$\begin{aligned}\{d\sigma\}&=[D_e]\cdot\{d\varepsilon^e\}\\&=[D_e]\cdot\{d\varepsilon\}-[D_e]\cdot(\{d\varepsilon^s\}+\{d\varepsilon^c\})\\&=[D_e]\cdot\{d\varepsilon\}-[D_e]\cdot[T](\{E_i^s\}\cdot dX+\{E_i^c\}\cdot d\sigma_m)\end{aligned} \tag{40}$$

Substituting Eq. (40) into Eqs. (14) and (29), dX and $d\sigma_m$ are represented as

$$\begin{aligned}dX&=\{A\}^T\cdot\{d\sigma\}\\&=\{A\}^T\cdot[D_e]\cdot\{d\varepsilon\}-\{A\}^T\cdot[D_e]\cdot[T]\cdot(\{E_i^s\}\cdot dX+\{E_i^c\}\cdot d\sigma_m)\end{aligned} \tag{41}$$

$$\begin{aligned}d\sigma_m&=\{B\}^T\cdot\{d\sigma\}\\&=\{B\}^T\cdot[D_e]\cdot\{d\varepsilon\}-\{B\}^T\cdot[D_e]\cdot[T]\cdot(\{E_i^s\}\cdot dX+\{E_i^c\}\cdot d\sigma_m)\end{aligned} \tag{42}$$

Eqs. (41) and (42) are rearranged as follows:

$$P_1\cdot dX+P_2\cdot d\sigma_m=\{A\}^T\cdot[D_e]\cdot\{d\varepsilon\} \tag{43}$$

$$Q_1\cdot dX+Q_2\cdot d\sigma_m=\{B\}^T\cdot[D_e]\cdot\{d\varepsilon\} \tag{44}$$

where

$$\left.\begin{aligned}P_1&=1+\{A\}^T\cdot[D_e]\cdot[T]\cdot\{E_i^s\}\\P_2&=\{A\}^T\cdot[D_e]\cdot[T]\cdot\{E_i^c\}\\Q_1&=\{B\}^T\cdot[D_e]\cdot[T]\cdot\{E_i^s\}\\Q_2&=1+\{B\}^T\cdot[D_e]\cdot[T]\cdot\{E_i^c\}\end{aligned}\right\} \tag{45}$$

i) In the case of $dX>0$ and $d\sigma_m>0$: dX and $d\sigma_m$ are expressed as follows from Eqs. (43) and (44):

$$dX=\frac{(Q_2\cdot\{A\}^T-P_2\cdot\{B\}^T)\cdot[D_e]\cdot\{d\varepsilon\}}{P_1Q_2-P_2Q_1} \tag{46}$$

$$d\sigma_m=\frac{(P_1\cdot\{B\}^T-Q_1\cdot\{A\}^T)\cdot[D_e]\cdot\{d\varepsilon\}}{P_1Q_2-P_2Q_1} \tag{47}$$

Substituting Eqs. (46) and (47) into Eq. (40), the constitutive equation can be given in an explicit form as follows:

$$\begin{aligned}\{d\sigma\}&=\left([D_e]-[D_e]\cdot[T]\cdot\{E_i^s\}\cdot\frac{Q_2\cdot\{A\}^T-P_2\cdot\{B\}^T}{P_1Q_2-P_2Q_1}\cdot[D_e]-[D_e]\cdot[T]\cdot\{E_i^c\}\cdot\frac{P_1\cdot\{B\}^T-Q_1\cdot\{A\}^T}{P_1Q_2-P_2Q_1}\cdot[D_e]\right)\cdot\{d\varepsilon\}\\&\equiv[D]\cdot\{d\varepsilon\}\end{aligned} \tag{48}$$

ii) In the case of $dX>0$ and $d\sigma_m\leqq0$: As the plastic strain increments due to consolidation $\{d\varepsilon^c\}$ are not produced when $d\sigma_m\leqq0$, Eqs. (40) and (41) are rewritten as follows:

$$\{d\sigma\}=[D_e]\cdot\{d\varepsilon\}-[D_e]\cdot[T]\cdot\{E_i^s\}\cdot dX \tag{49}$$

$$P_1\cdot dX=\{A\}^T\cdot[D_e]\cdot\{d\varepsilon\} \tag{50}$$

Substituting Eq. (50) into Eq. (49), the following equation is obtained.

$$\{d\sigma\}=\left([D_e]-[D_e]\cdot[T]\cdot\{E_i^s\}\right.$$

$$\cdot\frac{\{A\}^T}{P_1}\cdot[D_e]\Big)\cdot\{d\varepsilon\}$$
$$\equiv[D]\cdot\{d\varepsilon\} \tag{51}$$

iii) In the case of $dX\leqq 0$ and $d\sigma_m>0$: As the plastic strain increments due to shear $\{d\varepsilon^s\}$ are not produced when $dX\leqq 0$, Eqs. (40) and (42) are rewritten as follows:

$$\{d\sigma\}=[D_e]\cdot\{d\varepsilon\}-[D_e]\cdot[T]\cdot\{E_i^c\}\cdot d\sigma_m \tag{52}$$

$$Q_2\cdot d\sigma_m=\{B\}^T\cdot[D_e]\cdot\{d\varepsilon\} \tag{53}$$

Substituting Eq. (53) into Eq. (52), the following equation is obtained.

$$\{d\sigma\}=\Big([D_e]-[D_e]\cdot[T]\cdot\{E_i^c\}\cdot\frac{\{B\}^T}{Q_2}\cdot[D_e]\Big)\cdot\{d\varepsilon\}$$
$$\equiv[D]\cdot\{d\varepsilon\} \tag{54}$$

iv) In the case of $dX\leqq 0$ and $d\sigma_m\leqq 0$: In this case, $\{d\varepsilon^s\}=0$ and $\{d\varepsilon^c\}=0$, so the constitutive equation is expressed as follows:

$$\{d\sigma\}=[D_e]\cdot\{d\varepsilon\}\equiv[D]\cdot\{d\varepsilon\} \tag{55}$$

Failure Criterion of Soils

The failure criterion employed here has been derived from the concept of Spatial Mobilized Plane, and expressed as follows (Matsuoka and Nakai, 1974, 1977):

$$\frac{\tau_{SMP}}{\sigma_{SMP}}=\sqrt{\frac{J_1J_2-9J_3}{9J_3}}=\text{const.} \tag{56}$$

or

$$\frac{J_1\cdot J_2}{J_3}=\text{const.} \tag{57}$$

Fig. 3 shows this criterion in terms of the relation between the internal friction angle $\phi=\sin^{-1}\{(\sigma_1-\sigma_3)/(\sigma_1+\sigma_3)\}$ and $b=(\sigma_2-\sigma_3)/(\sigma_1-\sigma_3)$. The internal friction angle ϕ calculated from Eq. (56) or (57) has the same value under triaxial compression ($b=0.0$) and triaxial extension ($b=1.0$), and has higher values under three different principal stresses. The validity of this criterion has been confirmed by true triaxial test data (Nakai and Matsuoka, 1980, 1983). Now, in the present analysis, the behavior of soils after failure which have resistance to consolidation (increase in mean principal stress) but have no resistance to shear (increase in stress ratio) is approximately expressed by enlarging the values of the soil parameter γ_0^* of $\{E_i^s\}$ in Eq. (16).

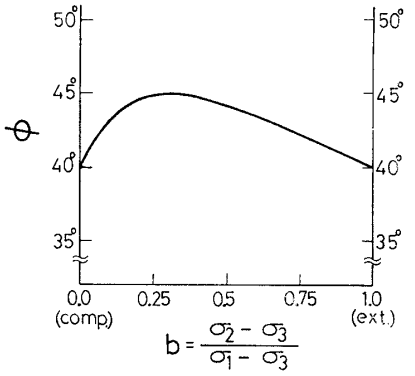

Fig. 3. Failure criterion based on SMP

ANALYSES OF SOIL ELEMENT TESTS AND COMPARISONS WITH EXPERIMENTAL RESULTS

The validity of the proposed constitutive equation is discussed here by analyzing various kinds of soil element tests. Tables 1 and 2 show all of the soil parameters of the medium dense Toyoura sand (initial void ratio $e_0\cong 0.68$) and the normally consolidated Fujinomori clay used in analyses, respectively. As these sand and clay are the same as in the previous paper by Nakai and Matsuoka (1983), the reader should refer to

Table 1. Soil parameters for Toyoura sand used in analysis

λ^*		0.9
μ^*		0.27
μ'^*		0.41
γ_0^*	γ_{0i}^*	0.10%
	C_d^*	0.066%
	σ_{mi}	98 kN/m² (1.0 kgf/cm²)
$C_c/(1+e_0)$		0.928×10^{-2}
$C_s/(1+e_0)$		0.578×10^{-2}
K_0		0.45
ν_e		0.3
$\phi_{(comp.)}$		40°

Table 2. Soil parameters for Fujinomori clay used in analysis

λ^*		0.9
μ^*		0.42
μ'^*		0.60
γ_0^*	γ_{0i}^*	3.3%
	C_d^*	0.0%
	σ_{mi}	
$C_c/(1+e_0)$		11.70×10^{-2}
$C_s/(1+e_0)$		1.60×10^{-2}
K_0		0.5
ν_e		0.3
$\phi_{(comp.)}$		34°

the paper for the details of samples and the test procedure. In Tables 1 and 2, the parameters λ^*, μ^*, μ'^* and γ_0^*, which are concerned with the shear component, are determined from constant mean principal tests under triaxial compression (Nakai and Matsuoka, 1983). $C_c/(1+e_0)$ and $C_s/(1+e_0)$ are determined from isotropic consolidation tests. K_0 value and ν_e are estimated from the results of anisotropic consolidation tests and unloading stress-strain relationship in shear tests, respectively. The internal friction angle under triaxial compression, $\phi_{(comp.)}$, is determined from the shear test. The failure criterion in Fig. 3 is the one for this medium dense Toyoura sand ($\phi_{(comp.)}=40°$).

Comparison between Analytical and Experimental Results of Element Tests on Sand

Fig. 4 shows the observed values (plots) and the calculated values (lines) for the triaxial compression and triaxial extension tests on the sand under a constant mean principal stress $\sigma_m=392\,kN/m^2$, with respect to the relation between the principal stress ratio (σ_1/σ_3) and the principal strains (ε_1 and ε_3). In this figure, the open plots and the solid lines denote the results in the triaxial compression condition, and the solid plots and the broken lines with dots denote the results in the triaxial extension condition. The analytical results explain well the ob-

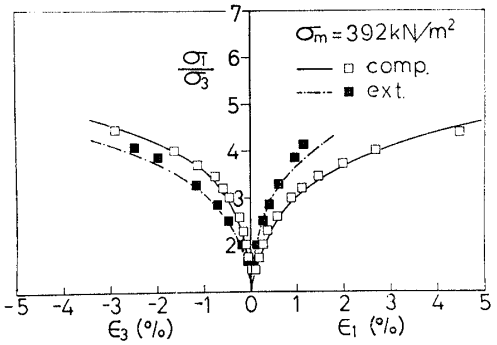

Fig. 4. Principal stress ratio vs. principal strains in triaxial compression and extension tests under constant mean principal stress

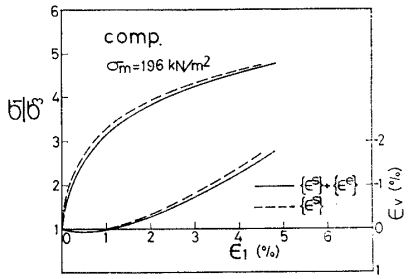

Fig. 5. Calculated stress-strain curves under constant mean principal stress

served values of shear tests. By the way, Fig. 5 compared the results calculated by the constitutive equation (the solid curves) in which the plastic component due to shear $\{d\varepsilon^s\}$ and elastic component $\{d\varepsilon^e\}$ are taken into consideration with the analytical results of $\{d\varepsilon^s\}$ alone (the broken curves). Since the difference between these two curves is relatively small, it is not a serious problem that the soil parameters (λ^*, μ^*, μ'^* and γ_0^*) concerning the shear component are determined without considering the elastic strains as do in the previous paper (Nakai and Matsuoka, 1983). The comparison between the analytical results and the observed values in the other shear tests, e. g., true triaxial tests, are not described here, since these comparisons were shown in the previous paper.

Next, analytical and experimental results of consolidation tests will be discussed. Figs. 2(a) and (b) described before present the results of the isotropic and anisotropic con-

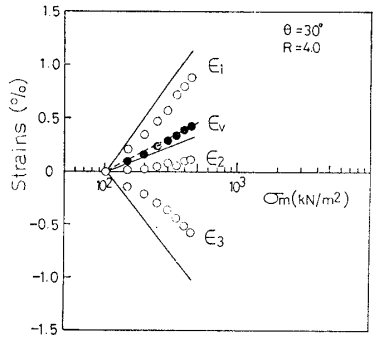

Fig. 6. Volumetric strain and principal strains vs. mean principal stress in true triaxial test (θ=30°) under constant principal stress ratio (R=4.0)

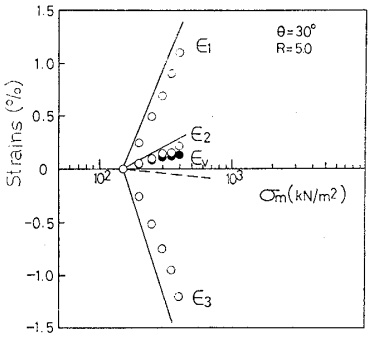

Fig. 7. Volumetric strain and principal strains vs. mean principal stress in true triaxial test (θ=30°) under constant principal stress ratio (R=5.0)

solidation tests. In these figures, the solid lines represent the analytical results by the constitutive equation. As is seen from these figures, the analytical results explain well the observed dilatancy behavior under anisotropic consolidation. It also appears that the principal stress ratio at which no volumetric strain is produced ($d\varepsilon_v$=0) is between 3 and 4 under triaxial compression condition, and is greater than 4 under triaxial extension condition. Figs. 6 and 7 indicate the observed values (plots) and the analytical results (lines) of the anisotropic consolidation tests at the major-minor principal stress ratio R=4 and R=5, respectively, under three different principal stresses. Here, θ=30° represents that the stress condition exists on a linear

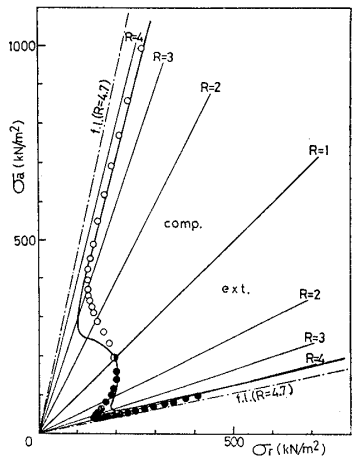

Fig. 8. Effective stress paths in undrained triaxial compression and extension tests

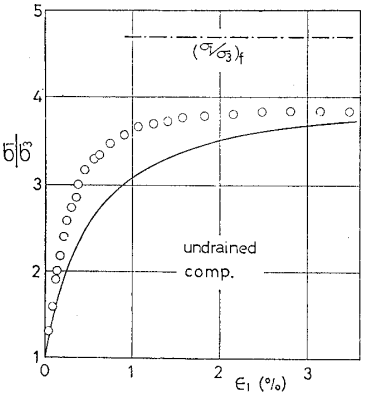

Fig. 9. Effective principal stress ratio vs. major principal strain in undrained triaxial compression test

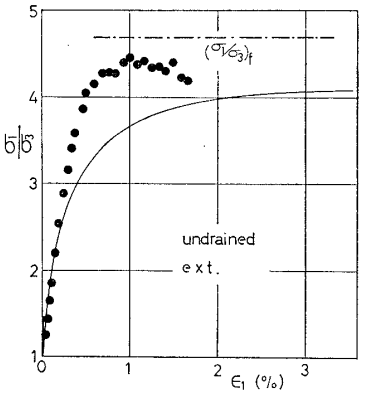

Fig. 10. Effective principal stress ratio vs. major principal strain in undrained triaxial extension test

line which makes 30 deg. away from the σ_1-axis on the octahedral plane, and there is the following relation among three principal stresses.

$$\sigma_2=(\sigma_1+\sigma_3)/2 \qquad (58)$$

The open circles and the solid lines in these figures denote the observed and calculated three principal strains (ε_1, ε_2 and ε_3) respectively, and the solid circles and the broken lines represent the observed and calculated volumetric strain (ε_v). It is seen from Figs. 6 and 7 that the analytical results using the soil parameters determined by the triaxial compression tests nearly explain the anisotropic consolidation behavior of soil under three different principal stresses, though there are some differences between the analytical and the observed results.

Fig. 8 shows the effective stress paths in undrained shear tests on the Toyoura sand under triaxial compression and triaxial extension conditions (initial confining pressure is 196 kN/m^2), and Figs. 9 and 10 indicate the stress-strain relationships of the same tests. In these figures, the plots represent the observed values and the solid lines the analytical results. The observed undrained stress paths do not reach the failure lines obtained from drained tests which are represented by the broken lines with dots, but converge to the above mentioned anisotropic consolidation paths that satisfy the condition of $d\varepsilon_v=0$ (see Figs. 2(a) and (b)). Therefore, the undrained strength ϕ' is smaller than the drained strength ϕ_d for the soil with positive dilatancy. These observed values also show that $\phi'_{(\text{comp.})}$ is smaller than $\phi'_{(\text{ext.})}$, though $\phi_{d(\text{comp.})}$ and $\phi_{d(\text{ext.})}$ are indentical. The results calculated by the proposed constitutive equation can explain such characteristics of the observed values.

Comparison between Analytical and Experimental Results of Element Tests on Clay

Figs. 11 and 12 indicate the analytical results (solid and broken lines) and the observed values (plots) of the triaxial compression and triaxial extension tests on the normally consolidated Fujinomori clay, respectively, in terms of the relation among the major-minor principal stress ratio (σ_1/σ_3), the major principal strain (ε_1) and the volumetric strain (ε_v). In these figures, the solid lines and circular plots denote the results of constant mean principal stress tests, and the broken lines and quadrilateral plots express the results of constant minor principal stress tests. It is obvious that the proposed constitutive equation explains the behavior of clay under various stress paths uniquely in the same manner as those of sand. It can also be seen that the principal stress ratio $(\sigma_1/\sigma_3)_f$ at failure is almost 3.5 (internal friction angle $\phi_d=34°$) regardless of the stress paths.

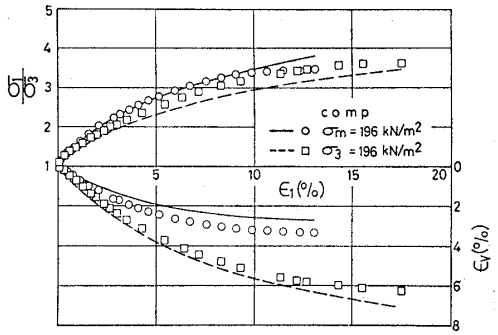

Fig. 11. Principal stress ratio vs. major principal strain vs. volumetric strain in triaxial compression tests on clay

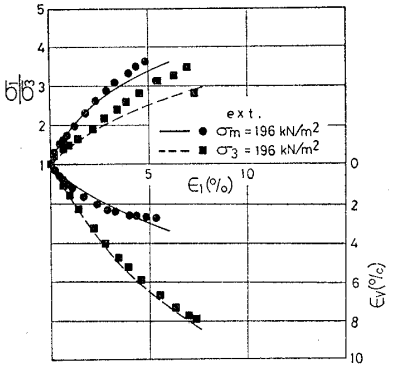

Fig. 12. Principal stress ratio vs. major principal strain vs. volumetric strain in triaxial extension tests on clay

Analyses of Plane Strain Tests and Simple Shear Test on Sand

Fig. 13 shows the analytical results of

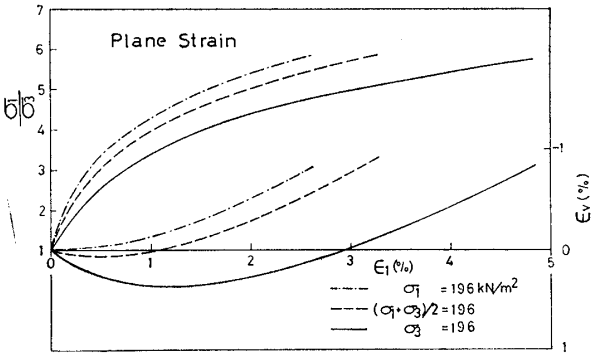

Fig. 13. Calculated stress-strain curves under plane strain condition

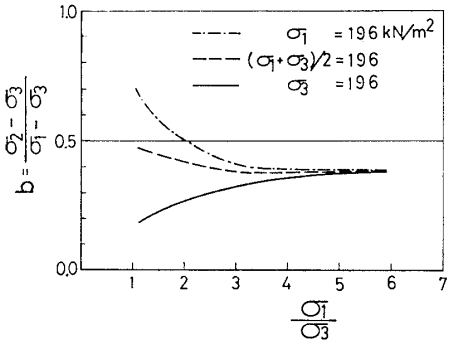

Fig. 14. Calculated variations of b-value under plane strain condition

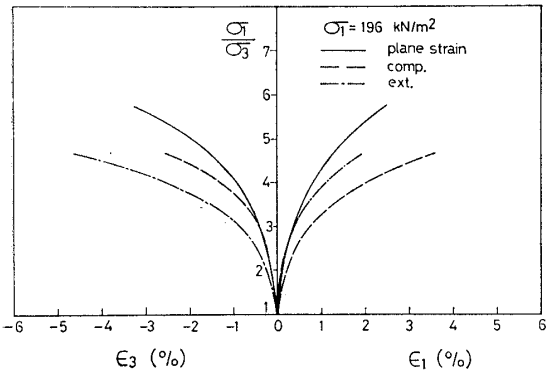

Fig. 15. Calculated stress-strain curves in plane strain, triaxial compression and triaxial extension tests under constant major principal stress

σ_1=const., $(\sigma_1+\sigma_3)/2$=const. and σ_3=const. tests under plane strain condition, with respect to the relation among σ_1/σ_3, ε_1 and ε_v. As shown here, the analytical results represent the change in soil dilatancy due to the difference of stress paths. Fig. 14 indicates the analytical variation of a parameter $b=(\sigma_2-\sigma_3)/(\sigma_1-\sigma_3)$ with an increase

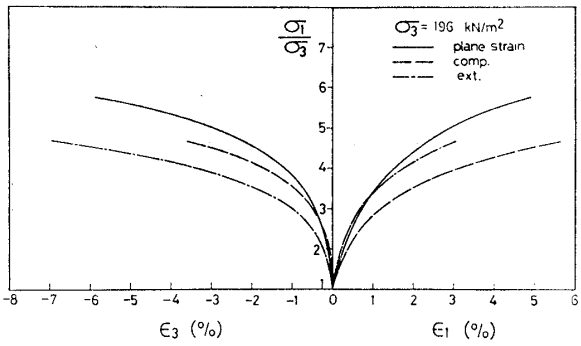

Fig. 16. Calculated stress-strain curves in plane strain, triaxial compression and triaxial extension tests under constant minor principal stress

in σ_1/σ_3 in the same test as in Fig. 13, where $b=0.0$ is the triaxial compression condition and $b=1.0$ the triaxial extension condition. It appears from this figure that the analytical results of b are different depending on the stress paths at the low stress ratio, but converge to a certain value between 0.3 and 0.4 as the stress ratio increases. Such analytical results correspond with the experimental results by the authors (Nakai and Matsuoka, 1980, 1983), and Lade and Duncan (1973).

Figs. 15 and 16 show the analytical results of plane strain, triaxial compression and triaxial extension tests on the sand under constant major principal stress and constant minor principal stress, respectively, in terms of the relation between σ_1/σ_3 and (ε_1 and ε_3). In these figures, each end of the calculated curves represents the stress condition at failure which is determined from the failure criterion based on the SMP in Fig. 3. It is seen from these figures that while the stress ratio at failure $(\sigma_1/\sigma_3)_f$ under both triaxial compression and triaxial extension conditions is 4.6 from $\phi_{(\text{comp.})}=\phi_{(\text{ext.})}=40°$, $(\sigma_1/\sigma_3)_f$ under plane strain condition becomes almost 5.7 (expressed in internal friction angle, $\phi_{(\text{plane strain})}=44.5°$). Yamaguchi et al. (1976) reported that $\phi_{(\text{plane strain})}$ becomes 46° when $\phi_{(\text{comp.})}=41°$, on the basis of experimental results of triaxial compression and plane strain tests on the Toyoura sand ($e_0\cong 0.66$) which is a little denser than that assumed here ($e_0\cong 0.68$). The present analytical results ($\phi_{(\text{plane strain})}=44.5°$ when

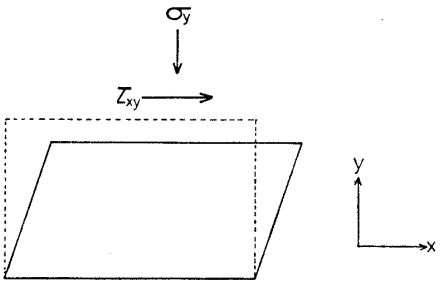

Fig. 17. Analytical model for simple shear test

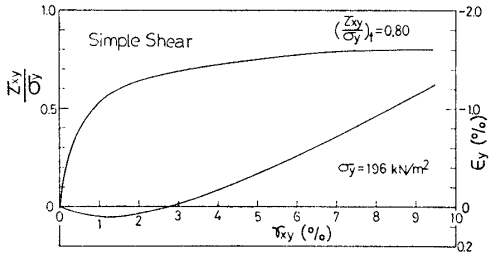

Fig. 18. Calculated stress-strain curve in simple shear test

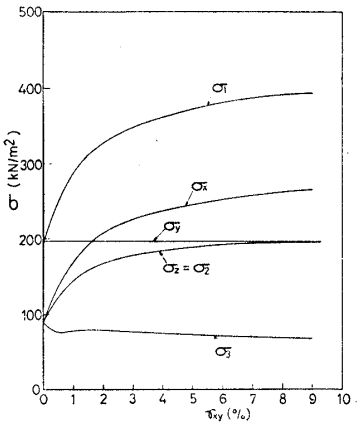

Fig. 19. Calculated variations of normal stresses (σ_x, σ_y and σ_z) and principal stresses (σ_1, σ_2 and σ_3)

$\phi_{(comp.)}=40°$) also corresponds to this experimental evidence.

Next, analysis of simple shear test will be described. As shown in Fig. 17, a state of simple shear is produced by forcing the upper part of the element to deflect in the direction of the x-axis. The z-axis is taken in the direction perpendicular to the x-y plane, and a plane strain condition is assumed where the strain in direction of the z-axis (ε_z) is zero. The initial condition of the element is

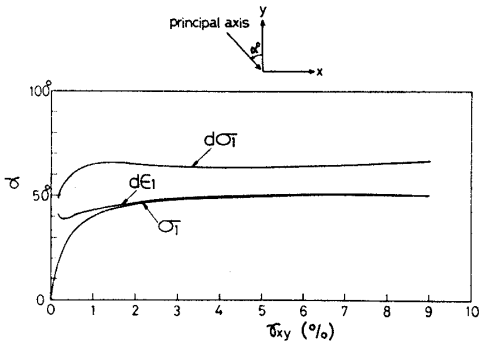

Fig. 20. Calculated direction of axes of major principal strain increment ($d\varepsilon_1$), major principal stress (σ_1) and major principal stress increment ($d\sigma_1$) in simple shear test

assumed to be a K_0-consolidation condition ($\sigma_y=196$ kN/m², $\sigma_x=\sigma_z=K_0\cdot\sigma_y=88.2$ kN/m²). Fig. 18 shows the analytical results of simple shear test with respect to the relation among the shear-normal stress ratio (τ_{xy}/σ_y), the shear strain (γ_{xy}) and the normal strain (ε_y). Fig. 19 indicates the variations of the three normal stresses (σ_x, σ_y and σ_z) and the three principal stresses (σ_1, $\sigma_2=\sigma_z$ and σ_3) obtained in analysis. It is seen from Fig. 18 that the shear-normal stress ratio at failure $(\tau_{xy}/\sigma_y)_f$ is 0.80, and the internal friction angle calculated by the equation $\phi_{(simple\ shear)}=\tan^{-1}(\tau_{xy}/\sigma_y)_f$ is 38.6°. By the way, at this time the principal stress ratio $(\sigma_1/\sigma_3)_f$ is almost 5.7 from Fig. 19, and corresponds with the value of plane strain tests in Figs. 15 and 16 mentioned before ($(\sigma_1/\sigma_3)_f=5.7$, $\phi_{(plane\ strain)}=44.5°$). When summerizing these analytical results, it is clear that the internal friction angle of simple shear test, $\phi_{(simple\ shear)}=38.6°$, which is determined only from τ_{xy} and σ_y, is smaller than that of triaxial compression test ($\phi_{(comp.)}=40°$), though a simple shear test is one of the element tests under plane strain condition. Now, as shown in Fig. 19, the mean principal stress $\sigma_m=(\sigma_x+\sigma_y+\sigma_z)/3$ in the simple shear test becomes large as the shear strain increases, because σ_x and σ_z gradually increase in spite of $\sigma_y=$ const. Therefore, the stress condition of the simple shear test may be fairly different from the pure shear condition. Ochiai (1975) indicated that the minor principal stress σ_3 did

not change in a direct shear test or a simple shear test, on the basis of the following equation by Oda and Konishi (1974).

$$\frac{\tau_{xy}}{\sigma_y}=\kappa\cdot\tan\psi \qquad (59)$$

where ψ is the angle between the y-axis and σ_1-axis, and κ the material constant. According to the analytical results in Fig. 19, this Ochiai's suggestion might be almost appropriate.

Fig. 20 shows the analytical direction of the axes of the major principal strain increment ($d\varepsilon_1$), the major principal stress (σ_1) and the major principal stress increment ($d\sigma_1$) in the simple shear test, where the direction angle α is taken positive anticlockwise as indicated in the upper part of the figure. It appears from this figure that the direction of $d\varepsilon_1$ is between the direction of σ_1 and the direction of $d\sigma_1$ at small strains (at the low stress ratio), but converge to the direction of σ_1 as the shear strain becomes large. This is due to the fact that as the stress ratio increases, the plastic strain becomes large in comparison with the elastic strain, because it is assumed in analysis that the plastic principal strain increment and the principal stress are identical in direction, and the elastic principal strain increment and the principal stress increment are identical in direction. This analytical result also corresponds to the experimental result of the simple shear test on a sand by Roscoe et al. (1967) shown in Fig. 21.

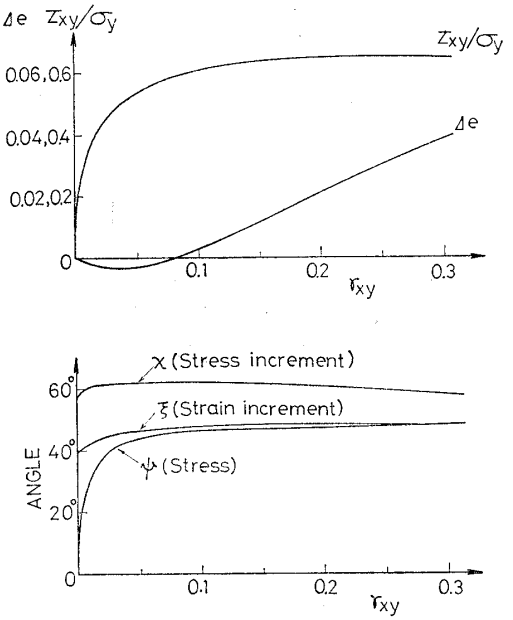

Fig. 21. Observed stress-strain curve and direction of axes of major principal strain increment (ξ), major principal stress (ψ) and major principal stress increment (χ) (after Roscoe, Bassett and Cole (1967))

ANALYSIS OF SOIL FOUNDATION WITH STRIP LOAD

Finite element analyses are performed for the case that a uniform strip load is imposed on a model foundation under plane strain condition. The model foundation has a depth of 24 m and a distance of 34 m from the center of the load, and is divided into 99 quadrilateral elements (120 nodal points) as shown in Fig. 22. The bottom boundary is assumed to be fixed, and the lateral boundary is assumed to be free only in the vertical direction. The half width of the strip load is 4 m. The material of the soil foundation is assumed to be the afore mentioned Toyoura sand, and the initial stress is calculated from the unit weight of the sand $\gamma_t=15.5\,\mathrm{kN/m^2}$ and the coefficient of earth pressure at rest $K_0=0.45$. The loading surface is assumed to be smooth. The computation is carried out with the incremental procedure by using the proposed constitutive equation. The accuracy of the computation is considered to be satisfactory, because there is no significant difference between the present computed results

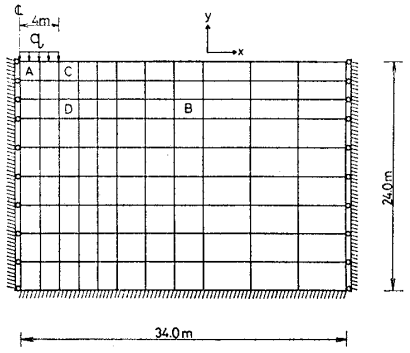

Fig. 22. Finite element mesh of soil foundation with uniform strip load

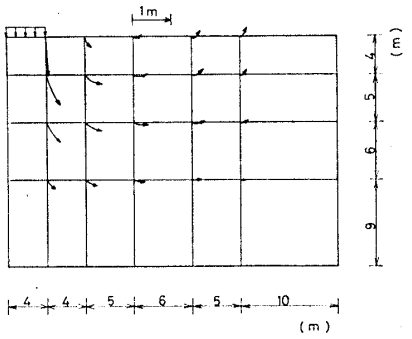

Fig. 23. Computed displacement vectors

and the results computed with a halved incremental load.

Fig. 23 shows the computed displacement vectors at several points in the soil foundation when the loading pressure q changes from 0 to 13,034 kN/m² which is the pressure just before the solution of the simultaneous equation diverges. It is seen from this figure that the displacements in the lateral direction become relatively large as the loading pressure increases.

Figs. 24(a), (b), (c) and (d) show the computed distributions of local factors of safety in the soil foundation at the loading pressure q=6,762 kN/m², 9,898 kN/m², 11,466 kN/m² and 13,034 kN/m², respectively. The factor of safety F. S. is defined as F. S. $=(\tau_{SMP}/\sigma_{SMP})_f/(\tau_{SMP}/\sigma_{SMP})$, where $(\tau_{SMP}/\sigma_{SMP})_f$ represents the shear-normal stress ratio on the SMP at failure. The zone where local factors of safety are relatively low develops mainly downward when the loading pressure q is not very high as shown in Fig. 24(a), but as q increases, the zone expands not only downward but also laterally. And it is interesting that this zone resembles the slip surface obtained by the Terzaghi's bearing capacity theory in shape, as shown in Figs. 24(c) and (d). It is also seen that the factor of safety of the zone beneath the strip load, which is considered to be a active wedge, is higher than that around this zone. For reference, the Terzaghi's ultimate bearing capacity pressure with smooth surface (Terzaghi, 1943) is nearly 3,500 kN/m² when $\phi=40°$, and is nearly 9,000 kN/m² when $\phi=44.5°$ which almost corresponds to the internal friction angle under plane strain condition calculated by using the failure criterion based on the SMP.

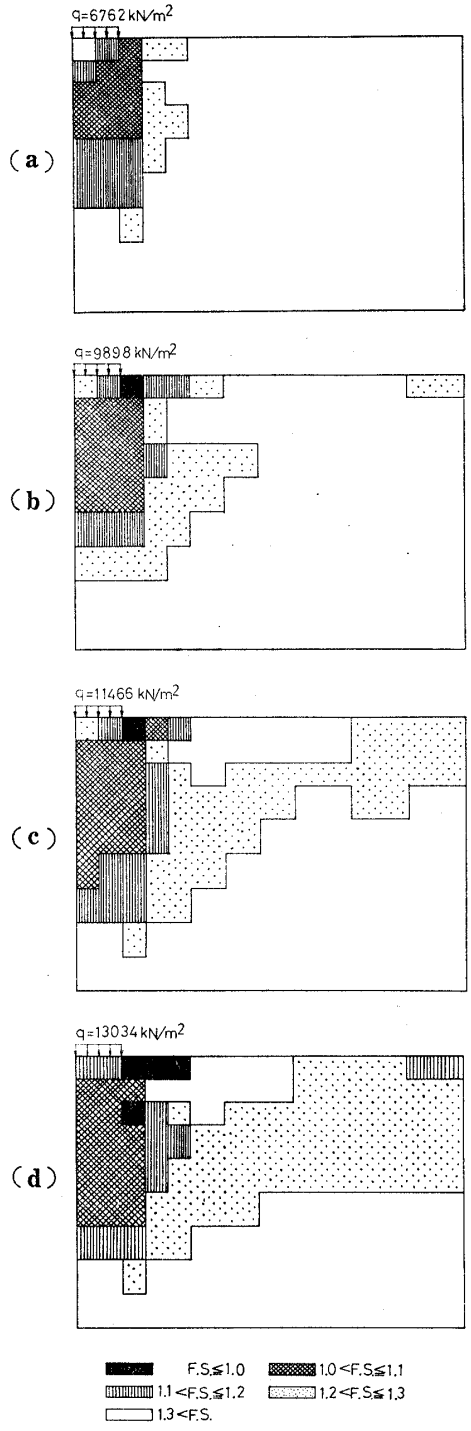

Fig. 24. Computed distributions of local factors of safety in soil foundation

Figs. 25 (a), (b), (c) and (d) show the changes in stress conditions of the elements A, B, C and D in Fig. 22, respectively, in

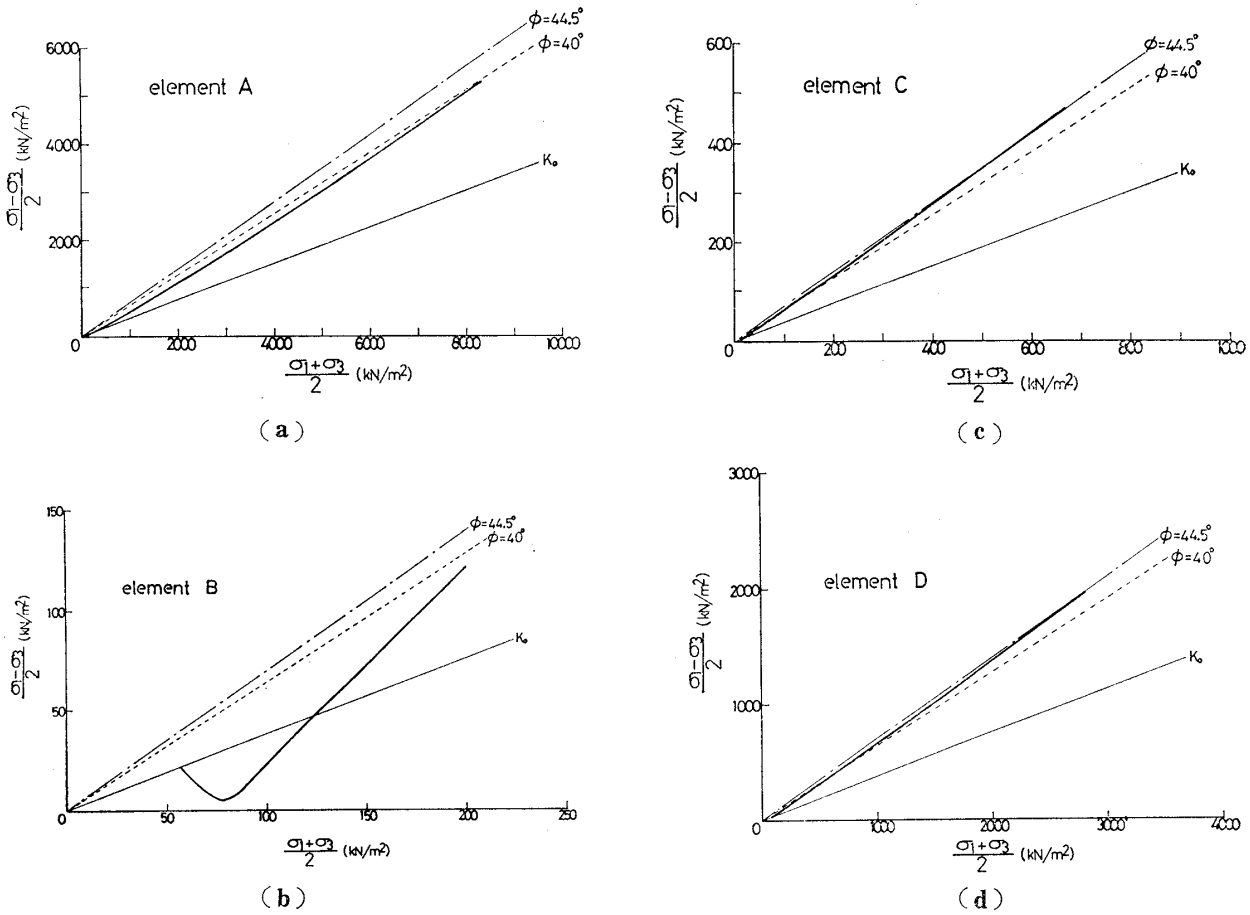

Fig. 25. Computed stress paths of elements (A, B, C and D) in Fig. 22

terms of the relation between the shear stress $(\sigma_1-\sigma_3)/2$ and the mean stress $(\sigma_1+\sigma_3)/2$. As shown in Fig. 25(a), although both shear and mean stresses of element A increase, the stress condition does not reach the failure line under plane strain condition which is represented by the broken line with dots. This corresponds to the experimental fact that the active wedge itself beneath the footing does not fail. It is seen from Fig. 25(b) that the stress ratio of element B in the passive zone decreases at first and then increases. Next, the stress conditions of elements C and D, which fail at the high loading pressure, move along the failure line after failure as shown in Figs. 25(c) and (d). These results indicate that the redistributions of stresses in the failed elements also are made properly in the present analysis.

Fig. 26 shows the computed distribution of local factors of safety in the case that the soil dilatancy due to anisotropic consolidation is not taken into consideration (E_2^* and G_2^* in Eq. (27) are assumed to be zero). In this case, the volumetric strain due to consolidation is given by Eq. (20) regardless of the stress ratio. What is obvious on comparing

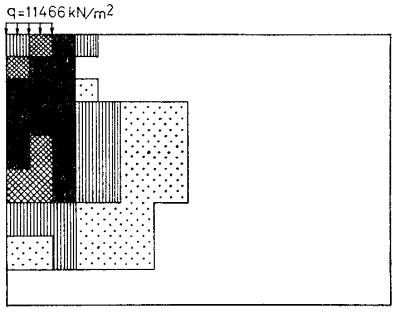

Fig. 26. Computed distribution of local factors of safety in soil foundation (in case that soil dilatancy due to anisotropic consolidation is not considered)

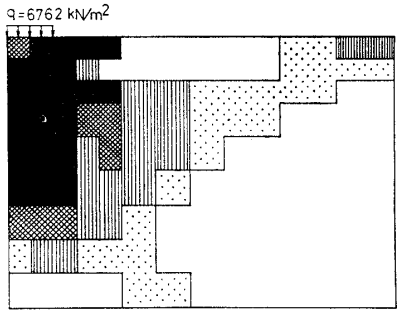

Fig. 27. Computed distribution of local factors of safety in soil foundation (in case that Mohr-Coulomb's failure criterion is used)

Fig. 26 with Fig. 24(c) is that in the case of Fig. 26 the zone of F. S. $\leqq$1. 3 does not expand so laterally as in Fig. 24(c), and the failure zone (F. S. $\leqq$1. 0) develops downward more widely. Thus, in such analysis of the bearing capacity problem where the mean stress of soil elements increases, the analytical results depends on whether the soil dilatancy due to anisotropic consolidation is considered or not.

Fig. 27 indicates the computed results when the Mohr-Coulomb's failure criterion is employed instead of the afore mentioned SMP failure criterion. Although in Fig. 24(a) the zone where local factors of safety are relatively low (F. S. $\leqq$1. 3) does not expand so widely, in Fig. 27 the zone of F. S. $\leqq$1. 3 is distributed more widely and more laterally, and the failure zone also develops. It is estimated on comparison of these two figures that the bearing capacity without considering the effect of the intermediate principal stress (in the case of employing Mohr-Coulomb's failure criterion) is much smaller than that in the case of employing the SMP failure criterion.

CONCLUSIONS

The main results of this paper are summerized as follows:

(1) A generalized constitutive equation is proposed on the basis of the idea that the total strain increments of soil consist of the plastic component due to shear, the plastic component due to consolidation and the elastic component. Both the plastic components due to shear and consolidation are provided by introducing the concept of "Spatial Mobilized plane (SMP)" and the amounts of strain increments based on the SMP.

(2) By using the proposed constitutive equation, analyses of various kinds of soil element tests are carried out; e. g. constant mean principal tests under triaxial compression and extension, isotropic and anisotropic consolidation tests under triaxial compression, extension and true triaxial conditions, undrained tests under triaxial compression and extension, plane strain tests, simple shear test and so on. It is confirmed by these analyses that the proposed constitutive equation can explain uniquely the deformation and strength characteristics of sand and clay under various stress paths in three-dimensional stresses. All the soil parameters of the proposed constitutive equation can be determined from shear and consolidation tests under triaxial compression condition.

(3) Finite element analyses of soil foundation with strip load are performed using this constitutive equation. It becomes clear that these analytical results explain well the various behaviors of deformation and failure of soil foundation which are known empirically. Especially, the computed zone where local factors of safety are relatively low expand not only downward but also laterally and distributed along the slip surface derived from the Terzaghi's bearing capacity theory.

ACKNOWLEDGEMENTS

The authors wish to thank Professor T. Yamauchi at Nagoya Institute of Technology and Professor T. Shibata at Kyoto University for their helpful support and encouragement. They are also indebted to Messrs. K. Kanaya, M. Suzuki, Y. Nomura and Y. Suzuki for their experimental assistance and useful discussion. This study was undertaken by the financial support of Grant-in-Aid for Encouragement of Young Scientist from the Ministry of Education, Science and Culture.

REFERENCES

1) Adachi, T. and Okano, M. (1974) : "A constitutive equation for normally consolidated clay," Soils and Foundations, Vol. 14, No. 1, pp. 55-73.
2) El-Sohby, M. A. (1969) : "Deformation of sand under constant stress ratio," Proc., 7 th ICSMFE, Vol. 1, pp. 111-119.
3) Lade, P. V. and Duncan, J. M. (1973) : "Cubical triaxial tests on cohesionless soil," Proc., ASCE, Vol. 99, No. SM 10, pp. 793-812.
4) Lade, P. V. and Duncan, J. M. (1975) : "Elastoplastic stress-strain theory for cohesionless soil," Proc., ASCE, Vol. 101, No. GT 10, pp. 1037-1053.
5) Matsuoka, H. and Nakai, T. (1974) : "Stress-deformation and strength characteristics of soil under three different principal stresses," Proc., JSCE, No. 232, pp. 59-70.
6) Matsuoka, H. and Nakai, T. (1977) : "Stress-strain relationship of soil based on the SMP," Proc., Specialty Session 9, 9 th ICSMFE, pp. 153-162.
7) Nakai, T. and Matsuoka, H. (1980) : "A unified law for soil shear behavior under three dimensional stress condition," Proc., JSCE, No. 303, pp. 65-77 (in Japanese).
8) Nakai, T. and Matsuoka, H. (1981) : "A unified law for soil deformation behavior under various stress paths," Proc., JSCE, NO. 306, pp. 23-34 (in Japanese).
9) Nakai, T. and Matsuoka, H. (1983) : "Shear behaviors of sand and clay under three-dimensional stress condition," Soils and Foundations, Vol. 23, No. 2, pp. 26-42.
10) Ochiai, H. (1975) : "The behavior of sands in direct shear tests," Jour. of JSSMFE, Vol. 15, No. 4, pp. 93-100 (in Japanese).
11) Ohta, H. (1971) : "Analysis of deformation of soils based on the theory of plasticity and its application to settlement of embankment," Dr. Eng. Thesis, Kyoto University.
12) Oda, M. and Konishi, J. (1974) : "Rotation of Principal stresses in granular materials during simple shear," Soils and Foundations, Vol. 14, No. 4, pp. 39-53.
13) Oka, F. (1981) : "Prediction of time-dependent behavior of clay," Proc., 10 th ICSMFE, Vol. 1, pp. 215-218.
14) Pender, M. J. (1977) : "A unified model for soil stress-strain behavior," Proc., Specialty Session 9, 9 th ICSMFE, pp. 213-222.
15) Prévost, J. H. (1978) : "Anisotropic undrained stress-strain behavior of clays," Proc., ASCE, Vol. 104, No. GT 8, pp. 1075-1090.
16) Roscoe, K. H., Bassett, R. H. and Cole, E. R. L. (1967) : "Principal axes observed during simple shear of a sand," Proc., Geotech. Conf., Oslo, pp. 231-237.
17) Roscoe, K. H., Schofield, A. N. and Thurairajah, A. (1963) : "Yielding of clays in states wetter than critical," Géotechnique, Vol. 13, No. 3, pp. 211-240.
18) Schofield, A. N. and Wroth, C. P. (1968) : Critical State Soil Mechanics, Mcgraw-Hill, London.
19) Sekiguchi, H. (1977) : "Rheological characteristics of clays," Proc., 9 th ICSMFE, Vol. 1, pp. 289-292.
20) Sekiguchi, H. and Ohta, H. (1977) : "Induced anisotropy and time dependency in clays," Proc., Specialty Session 9, 9 th ICSMFE, pp. 229-238.
21) Terzaghi, K. (1943) : Theoretical Soil Mechanics, John Wiley and Sons.
22) Yamada, Y., Yoshimura, N. and Sakurai, T. (1968) : "Plastic stress-strain matrix and its application for the solution of elastic-plastic problems by the finite element method," Int. Journ. Mech. Sci., Vol. 10, pp. 343-354.
23) Yamaguchi, H., Kimura, T. and Fujii, N. (1976) : "On the influence of progressive failure on the bearing capacity of shallow foundations in dense sand," Soils and Foundations, Vol. 16, No. 4, pp. 11-22.

APPENDIX

The Transformation Matrix [T] under Plane Strain Condition:

In the plane strain condition that the strain increment $d\varepsilon_z$ is zero and σ_3-axis coincides with z-axis in direction, there are following relations.

$$\left.\begin{aligned} l_z = m_z = 0 \\ n_z = 1 \\ n_x = n_y = 0 \end{aligned}\right\} \qquad \text{(A1)}$$

If the major and minor principal stresses in the $x-y$ plane are σ_1 and σ_2, respectively, and the angle β between σ_1-axis and x-axis is denoted as in Fig. A 1, β is given by the stresses (σ_x, σ_y and τ_{xy}) as follows:

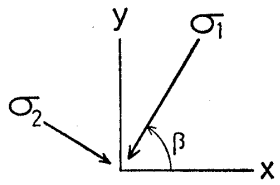

Fig. A 1. Definition of angle β between σ_1-axis and x-axis

$$\beta=\begin{cases}\dfrac{1}{2}\cdot\tan^{-1}\left(\dfrac{2\tau_{xy}}{\sigma_x-\sigma_y}\right) & (\sigma_x\geqq\sigma_y)\\ \dfrac{1}{2}\cdot\tan^{-1}\left(\dfrac{2\tau_{xy}}{\sigma_x-\sigma_y}\right)+\dfrac{\pi}{2} & (\sigma_x<\sigma_y)\end{cases} \tag{A 2}$$

Therefore, the transformation matrix $[T]$ in Eq. 17 is rewritten as follows under plane strain condition:

$$[T]=\begin{bmatrix}\cos^2\beta & \sin^2\beta & 0\\ \sin^2\beta & \cos^2\beta & 0\\ 0 & 0 & 1\\ \sin 2\beta & -\sin 2\beta & 0\\ 0 & 0 & 0\\ 0 & 0 & 0\end{bmatrix} \tag{A 3}$$